plastic instabilities[27–29] may incorporate a time dependence that may serve as a nonlinear temperature-dependent delay factor in dynamic triggering. We purpose that deep events can be remotely triggered by transient effects incorporating such nonlinear short-term delay mechanisms in regions where high stress may predominate, but where earthquakes have difficulty nucleating without external influences. □

Methods

Aftershock location

We combined teleseismic arrival times from the Preliminary Determination of Epicentres (PDE) with regional data from the SPANET network (Fig. 1) to constrain the location of the 2002 sequences. P, pP, sP and regional S arrival times were inverted using a hypocentroidal decomposition method that minimizes the effect of velocity heterogeneities along the ray paths[30]. Two stations of the Global Seismic Network (GSN), AFI and MSVF, and stations of the SPANET network, located at distances of about 5–13° (Fig. 1), recorded upgoing P and/or S phases that allowed better depth constraints.

Body-waveform inversion

Using global broadband data, we inverted for the source parameters of both mainshocks[21,31]. Global data were combined with recordings of the SPANET network to infer the focal mechanism of the larger (M_b >4.6) aftershocks with a grid search method that fits P and SH waveforms simultaneously.

Coulomb failure stress

The Coulomb failure stress change is expressed as $\Delta\sigma_f = \Delta\tau + \mu'\Delta\sigma$, where $\Delta\tau$ is the shear stress change on a fault (positive in the direction of fault slip), $\Delta\sigma$ is the normal stress change (positive for extension), and μ' is the apparent coefficient of friction, which includes the effects of pore pressure change. Failure is promoted if $\Delta\sigma_f$ is positive and inhibited if negative [1,32]. The Coulomb stress changes are computed in an elastic half-space using the finite-fault source model for the initial event which consists of three subfaults (Supplementary Table 3). For each subfault, an uniform slip distribution, consistent with the estimated average dislocation of 2 m, is used. Aftershocks located in the depth range between 579 km ad 623 km imply widths of about 40 km for the near vertical subfaults. In the calculations, we assumed a shear modulus of 11.6×10^{11} dyn cm^{-2}, appropriate for a depth of 571 km, and a Poisson's ratio of 0.24 for olivine, the dominant mineral in mantle. For the apparent coefficient of friction μ', we employed values ranging from 0.6 to 0.9. The general stress distribution was similar for all these values. The final models were computed for $\mu' = 0.7$.

Received 18 April; accepted 14 July 2003; doi:10.1038/nature01903.

1. King, G. C. P., Stein, R. S. & Lin, J. Static stress changes and the triggering of earthquakes. *Bull. Seismol. Soc. Am.* **84,** 935–953 (1994).
2. Harris, R. A. Introduction to special section: stress triggers, stress shadows, and implications for seismic hazard. *J. Geophys. Res.* **103,** 24347–24358 (1998).
3. Stein, R. S. The role of stress transfer in earthquake occurrence. *Nature* **402,** 605–609 (1999).
4. Hill, D. P. *et al.* Seismicity remotely triggered by the magnitude 7.3 Landers, California, earthquake. *Science* **260,** 1617–1623 (1993).
5. Harris, R. A. & Day, S. M. Dynamics of faults interaction: parallel strike-slip faults. *J. Geophys. Res.* **98,** 4461–4472 (1993).
6. Belardinelli, M. E., Cocco, M., Coutant, O. & Cotton, F. Redistribution of dynamic stress during coseismic ruptures: evidence for fault interaction and earthquake triggering. *J. Geophys. Res.* **104,** 14925–14945 (1999).
7. Kilb, D., Gomberg, J. & Bodin, P. Triggering of earthquake aftershocks by dynamic stresses. *Nature* **408,** 570–574 (2000).
8. Gomberg, J., Blanpied, M. L. & Beeler, N. M. Transient triggering of near and distant earthquakes. *Bull. Seismol. Soc. Am.* **87,** 295–309 (1997).
9. Frohlich, C. The nature of deep-focus earthquakes. *Annu. Rev. Earth Planet. Sci.* **17,** 227–254 (1989).
10. Green, H. W. & Houston, H. The mechanics of deep earthquakes. *Annu. Rev. Earth Planet. Sci.* **23,** 169–213 (1995).
11. Kirby, S. H., Stein, S., Okal, E. A. & Rubie, D. C. Metastable mantle phase transformations and deep earthquake in subducting oceanic lithosphere. *Rev. Geophys.* **34,** 261–306 (1996).
12. Wiens, D. A. Seismological constraints on the mechanism of deep earthquakes: temperature dependence of deep earthquake source properties. *Phys. Earth. Planet. Inter.* **127,** 145–163 (2001).
13. Tibi, R., Bock, G. & Wiens, D. A. Source characteristics of large deep earthquakes: constraint on the faulting mechanism at great depths. *J. Geophys. Res.* **108,** doi:101029/2002JB001948 (2003).
14. Jaeger, J.C. & Cook, N.G.W. *Fundamentals of Rock Mechanics* (Chapman and Hall, London, 1979).
15. Wiens, D. W. & McGuire, J. J. Aftershocks of the March 9, 1994, Tonga earthquake: the strongest known deep aftershock sequence. *J. Geophys. Res.* **105,** 19067–19083 (2000).
16. Cotton, F. & Coutant, O. Dynamic stress variations due to shear faults in a plane-layered medium. *Geophys. J. Int.* **128,** 676–688 1997).
17. Kisslinger, C. A review of theories of mechanisms of induced seismicity. *Eng. Geol.* **10,** 85–98 (1976).
18. Gomberg, J., Reasenberg, P. A., Bodin, P. & Harris, R. A. Earthquake triggering by seismic waves following the Landers and Hector Mine earthquakes. *Nature* **411,** 462–466 (2001).
19. Van der Hilst, R. D. Complex morphology of subducted lithosphere in the mantle beneath the Tonga trench. *Nature* **374,** 154–157 (1995).
20. Chen, W.-P. & Brudzinski, M. R. Evidence for a large-scale remnant of subducted lithosphere beneath Fiji. *Science* **292,** 2475–2479 (2001).
21. Tibi, R. *Untersuchungen der Ursache von Tiefherdbeben mit Hilfe von Breitbandseismogrammen. Scientific Technical Report STR00/08* (GeoForschungsZentrum Potsdam, Potsdam, 2000).
22. McGuire, J. J., Wiens, D. A., Shore, P. J. & Bevis, M. G. The March 9, 1994 (M_w 7.6), deep Tonga earthquake: rupture outside the seismically active slab. *J. Geophys. Res.* **102,** 15163–15182 (1997).
23. Hudnut, K. W., Seeber, L. & Pacheco, J. Cross-fault triggering in the November 1987 Superstition Hills earthquake sequence, Southern California. *Geophys. Res. Lett.* **16,** 199–202 (1989).
24. Freed, A. M. & Lin, J. Delayed triggering of the 1999 Hector Mine earthquake by viscoelastic stress transfer. *Nature* **411,** 180–183 (2001).
25. Pollitz, F. F. & Sacks, I. S. The 1995 Kobe, Japan, earthquake: a long-delayed aftershock of the offshore 1944 Tonankai and 1946 Nankaido earthquakes. *Bull. Seismol. Soc. Am.* **87,** 1–7 (1997).
26. King, G. C. P. & Cocco, M. Fault interaction by elastic stress changes: new clues from earthquake sequences. *Adv. Geophys.* **44,** 1–38 (2000).
27. Ogawa, M. Shear instability in a viscoelastic material as the cause of deep focus earthquakes. *J. Geophys. Res.* **92,** 13801–13810 (1987).
28. Hobbs, B. E. & Ord, A. Plastic instabilities: implications for the origin of intermediate and deep focus earthquakes. *J. Geophys. Res.* **93,** 10521–10521 (1988).
29. Karato, S., Riedel, M. R. & Yuen, D. A. Rheological structure and deformation of subducted slabs in the mantle transition zone: implications for mantle circulation and deep earthquakes. *Phys. Earth Plant. Inter.* **127,** 83–108 (2001).
30. Jordan, T. H. & Sverdrup, K. A. Teleseismic location techniques and their application to earthquake clusters in the South-Central Pacific. *Bull. Seismol. Soc. Am.* **71,** 1105–1130 (1981).
31. Nábělek, J. L., *Determination of Earthquake Source Parameters from Inversion of Body Waves.* PhD thesis, MIT (1984).
32. Toda, S., Stein, R. S., Reasenberg, P. A., Dieterich, J. H. & Yoshida, A. Stress transferred by the 1995 M_w = 6.9 Kobe, Japan, shock: effect on aftershocks and future earthquake probabilities. *J. Geophys. Res.* **103,** 24543–24565 (1998).
33. Engdahl, E. R., van der Hilst, R. & Buland, R. Global teleseismic earthquake relocation with improved travel times and procedures for depth determination. *Bull. Seismol. Soc. Am.* **88,** 722–742 (1998).
34. Gudmundsson, Ó. & Sambridge, M. A regionalized upper mantle (RUM) seismic model. *J. Geophys. Res.* **103,** 7121–7136 (1998).
35. Dziewonski, A. M., Chou, T.-A. & Woodhouse, J. H. Determination of earthquake source parameters from waveform data for studies of global and regional seismicity. *J. Geophys. Res.* **86,** 2825–2852 (1981).

Supplementary Information accompanies the paper on **www.nature.com/nature**.

Acknowledgements We thank D. Suetsugu and the operators of the SPANET network for their efforts, R. Stein for making his code available, and J. Conder and N. Kagotho for reading the manuscript. Waveforms data were supplied by the Incorporated Research Institutions for Seismology (IRIS), Geoscope, and GeoForschungsNetz (GEOFON). Arrival time data were obtained from the ISC and PDE (US Geological Survey). This research was supported by the National Science Foundation.

Competing interests statement The authors declare that they have no competing financial interests.

Correspondence and requests for materials should be addressed to R.T. (tibi@seismo.wustl.edu).

Xenoturbella is a deuterostome that eats molluscs

Sarah J. Bourlat[1], Claus Nielsen[2], Anne E. Lockyer[3], D. Timothy J. Littlewood[3] & Maximilian J. Telford[1]

[1]*University Museum of Zoology, Department of Zoology, Downing Street, Cambridge CB2 3EJ, UK*
[2]*Zoological Museum (University of Copenhagen), Universitetsparken 15, DK-2100 Copenhagen, Denmark*
[3]*Department of Zoology, The Natural History Museum, Cromwell Road, London SW7 5BD, UK*

***Xenoturbella bocki*, first described in 1949 (ref. 1), is a delicate, ciliated, marine worm with a simple body plan: it lacks a through gut, organized gonads, excretory structures and coelomic cavities. Its nervous system is a diffuse nerve net with no brain. *Xenoturbella*'s affinities have long been obscure and it was initially linked to turbellarian flatworms[1]. Subsequent authors considered it variously as related to hemichordates and echinoderms owing to similarities of nerve net and epidermal ultrastructure[2,3], to acoelomorph flatworms based on body plan and ciliary ultrastructure[4–6] (also shared by hemichordates[7]), or as among the most primitive of Bilateria[8]. In 1997 two papers seemed to solve this uncertainty: molecular phylogenetic**

analyses[9] placed *Xenoturbella* within the bivalve molluscs, and eggs and larvae resembling those of bivalves were found within specimens of *Xenoturbella*[10,11]. This molluscan origin implies that all bivalve characters are lost during a radical metamorphosis into the adult *Xenoturbella*. Here, using data from three genes, we show that the samples in these studies were contaminated by bivalve embryos eaten by *Xenoturbella* and that *Xenoturbella* is in fact a deuterostome related to hemichordates and echinoderms.

We carried out independent polymerase chain reaction (PCR) amplifications using ten different sets of primers for three genes (small subunit ribosomal DNA (*SSU*) and cytochrome oxidase 1 and 2 (*cox1* and *2*)) on two specimens of *Xenoturbella* collected from soft mud at a depth of 100 m near Kristineberg, Sweden. From each experiment we found sequences that were most similar to those from bivalve molluscs; in every case we also found another distinct sequence. Our contention that the molluscan sequences are derived from food ingested by *Xenoturbella* is supported by examination of the sequence evidence. Our molluscan-type *cox1* sequence is 97.2% similar at the nucleotide level (593 out of 610) to a sequence from the mollusc *Nucula tenuis* (found at Kristineberg); for comparison *N. tenuis* and congeneric *N. sulcata* are 75% similar. It seems extremely unlikely that *Xenoturbella*, with no molluscan features, could be this genetically similar to a bivalve mollusc. This result is echoed by analyses of a section of *SSU* (corresponding to positions 1500–1850 in *Homo sapiens SSU*) where we found two molluscan sequences, one identical to the published *Xenoturbella* sequence, the second identical to *N. sulcata SSU*. The most plausible explanation for these different sequences is that they derive from different bivalve molluscs that have been ingested by *Xenoturbella* as embryos or larvae. This idea is confirmed by experiments comparing *SSU* PCR products amplified from an intact animal with those in which we dissected away as much of the gut as possible from our specimen. In PCR experiments where mollusc-type sequences are distinguishable from alternative sequences by molecular mass, the concentration of the mollusc-type PCR product decreases in the sample with gut dissected out compared with the intact animal sample; the relative concentration of the alternative sequence increases when the sample contains less gut (Supplementary Information). We conclude from our experiments that the most likely explanation for the similarity to molluscs of some of our sequences and the sequences previously reported from *Xenoturbella* is that they derive from material in the gut and that the alternative sequences must therefore be from *Xenoturbella*.

Phylogenetic analyses[12,13] using our complete *Xenoturbella SSU* sequence place it within the deuterostomes (Fig. 1; 99% non-parametric bootstrap support (BP) and 100% posterior probability in a bayesian analysis (MB)). Although rooting the Bilateria using different outgroups results in different positions for the root (see Supplementary Information) we make the assumption that the deuterostomes (with or without *Xenoturbella*) are monophyletic. Within the deuterostomes *Xenoturbella* groups with the Ambulacraria (hemichordates and echinoderms) (92% BP, 100% MB) but is basal to both phyla (excluded from Ambulacraria 54% BP, 94% MB). A likelihood ratio test showed that there was significantly more support for positioning *Xenoturbella* within the deuterostomes than for positioning it at the base of the Bilateria or at the base of the deuterostomes ($P < 0.05$). Likelihood ratio tests did not reject the possibility that *Xenoturbella* is a basal hemichordate ($P < 0.061$) or a basal echinoderm ($P < 0.17$) although other information (see below) argues against these possibilities. In our best tree, the urochordates branched at the base of the deuterostomes. Excluding the urochordates from a monophyletic Chordata does not have strong support (76% BP, 86% MB) and a likelihood ratio test shows that our tree with paraphyletic chordates was not significantly better supported than a tree with monophyletic chordates ($P < 0.158$). The observed paraphyly of chordates seems most likely to be a result of the relatively long branches of the urochordates.

We also have nucleotide sequence from *Xenoturbella* correspond-

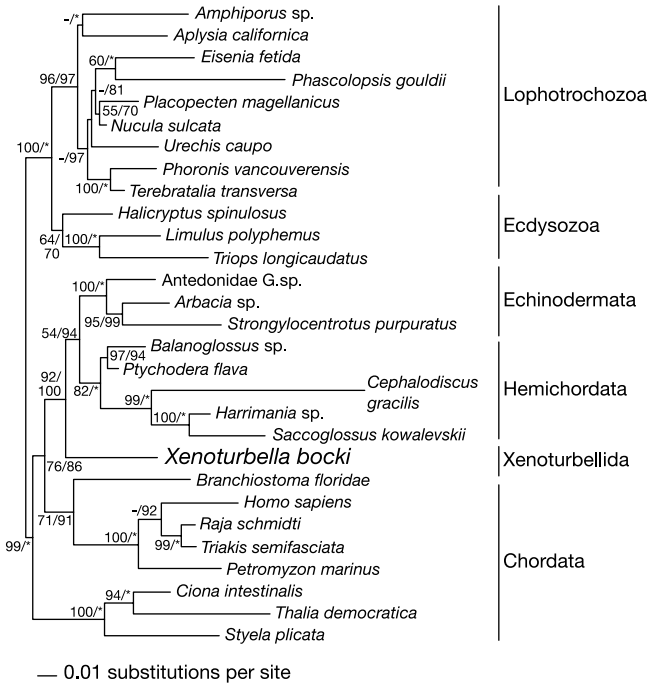

Figure 1 Best ML tree found using *SSU* sequences. *Xenoturbella* is within the deuterostomes basal to a clade containing the echinoderms and hemichordates. Values are non-parametric bootstrap (first) and MB posterior probabilities (second). MB values of 100 are represented by an asterisk to save space. Maximum parsimony and neighbour-joining analyses placed *Xenoturbella* in an identical position within deuterostomes. The tree has been rooted such that the deuterostomes are monophyletic. Positioning the root on *Xenoturbella* as suggested by rooting with one acoelomorph, *Meara*, would imply paraphyly of the deuterostomes and for this and other reasons is rejected (see Supplementary Information). Forcing *Xenoturbella* to the base of the deuterostomes is significantly less well supported according to likelihood ratio tests ($P < 0.05$). None of the included taxa had a statistically significant divergence from homogeneity of base composition.

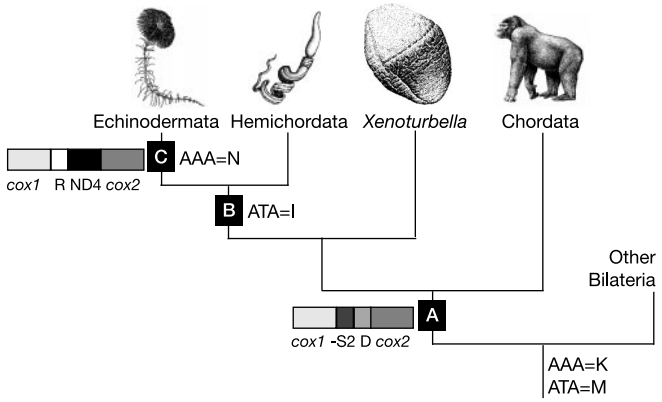

Figure 2 Position of *Xenoturbella* within the deuterostomes as suggested by our analyses of *SSU* and mitochondrial data. The distribution of synapomorphic molecular character states is indicated by a letter. A, monophyly of deuterostomes including *Xenoturbella* supported by common mitochondrial gene order; B, monophyly of Ambulacraria (hemichordates plus echinoderms) to the exclusion of *Xenoturbella* supported by one genetic code change; C, Monophyly of crown-group echinoderms supported by further genetic code change and gene order change.

ing to most of *cox1*, the 106 amino acids at the amino terminal of *cox2* and the sequence linking these two genes. Although phylogenetic analyses using *cox1* sequences are less reliable at this level of divergence than those of *SSU*, phylogenetic analyses of *cox1* sequences support our results from *SSU*, also placing *Xenoturbella* within the deuterostomes but in this case as the sister group of the hemichordate *Balanoglossus* (see Supplementary Information). These mitochondrial sequences provide us with two additional sources of information for testing the phylogenetic position of *Xenoturbella*–gene order and mitochondrial genetic codes.

Analyses of our mitochondrial sequences[14] show that there are two transfer RNA genes positioned between *Xenoturbella cox1* and *cox2*: *tRNA-S2* (anticodon UGA for serine) adjacent to *cox1* in the reverse orientation, followed by *tRNA-D* (anticodon GUC for aspartic acid) and then *cox2*. Of the metazoans studied so far this gene order is seen only in deuterostomes (cephalochordates, vertebrates and hemichordates; see http://www.jgi.doe.gov/programs/comparative/Mito_top_level.html) providing further evidence that *Xenoturbella* is a deuterostome (Fig. 2). A different gene arrangement is seen in echinoderms demonstrating that *Xenoturbella* is excluded from the crown group of the echinoderms.

An informative mitochondrial genetic code variant is also found in hemichordates and echinoderms[15] (and convergently in rhabditophoran Platyhelminthes). In both ambulacrarian phyla the codon ATA codes for isoleucine (I) rather than for methionine (M), as is the case in most other metazoans. Examination of *Xenoturbella cox1* and *cox2* following the method in ref. 15 shows that ATA codes for the standard metazoan M (see Supplementary Information). The lack of this hemichordate and echinoderm synapomorphy may suggest that *Xenoturbella* lies outside these two ambulacrarian clades (Fig. 2). There is some further support for this contention, albeit less compelling, from another alteration in mitochondrial genetic code. In echinoderms the codon AAA codes for asparagine (N) rather than lysine (K) as it does in most metazoans, and there has been a concomitant change in the echinoderm lysine tRNA anticodon from TTT to CTT. It has been proposed that the complete absence of the codon AAA from the hemichordate mitochondrial genome is an intermediate step in this reassignment and this is supported by the observation of the same change in the hemichordate lysine tRNA anticodon[16]. In contrast, our analyses show that in *Xenoturbella* the codon AAA codes for K as in most other Metazoa (see Supplementary Information).

Xenoturbella cox1 and partial *cox2* genes lack the codons AGA and AGG: the related serine codons AGC and AGT each occur five times. The absence of the AGG codon (if true of the whole *Xenoturbella* mitochondrial genome) is another more tentative link with the deuterostomes; this codon—which codes for serine in most metazoan mitochondria—is not found, or codes for an amino acid other than serine, in all deuterostome taxa apart from echinoderms.

Our results indicate that *Xenoturbella* is not a highly degenerate bivalve mollusc and that the evidence supporting this theory—molluscan eggs, larvae and gene sequences—can be best explained by concluding that *Xenoturbella* eats nuculid mollusc adults, eggs and pericalymma larvae. Notably, both *N. tenuis* and *N. sulcata* are common in the same habitat as *Xenoturbella*. The published *Xenoturbella SSU* sequence must derive from another of the 109 species of bivalve mollusc found around Kristineberg.

Figure 2 summarizes the relationship of *Xenoturbella* to the other deuterostome taxa suggested by our analyses of *SSU* sequences: in interpreting this tree we make the assumption that the chordates are monophyletic. This scheme of relationships could suggest that the simplicity of *Xenoturbella* represents the primitive form of the deuterostomes and even that this simplicity derives directly from more basal taxa such as the acoelomorphs with which *Xenoturbella* has been linked[5,6]. It is also possible that *Xenoturbella* is more closely related to one or other of the two ambulacrarian clades, although this is not seen in our best tree and our mitochondrial code data provide some evidence against this. Whether *Xenoturbella* is basal to the Ambulacraria or sister group to either the hemichordates or the echinoderms, consideration of characters shared by the Ambulacraria and the chordates such as coelomic cavities, complete gut with separate mouth and anus and gill slits, suggest that these characters have been secondarily lost by *Xenoturbella*. This would mean that at least some aspects of its simplicity are derived. Future studies of the embryology of *Xenoturbella* would be expected to reveal further characters commonly found in deuterostomes such as radial cleavage, a ciliated larva and perhaps some degree of left/right asymmetry during development as seen in the ontogeny both of chordates and of hemichordates and echinoderms[17].

Because of the pivotal phylogenetic position of *Xenoturbella* as a close relative of the hemichordates and echinoderms and an outgroup to the chordates, future studies of the genetics, morphology and embryology of *Xenoturbella* have the potential to provide great insight into the evolution of the deuterostomes. *Xenoturbella* has previously been placed in the high-ranking taxon Xenoturbellida[1]. If future experiments show *Xenoturbella* to be the sister group of the Ambulacraria, as our evidence suggests, then Xenoturbellida would constitute a new phylum of deuterostome. □

Methods

See supplementary Information for specimens, PCR and sequencing primers, and PCR and sequencing methods.

Alignment

SSU sequences were downloaded already aligned according to secondary structure from Ribosomal Database Project II (http://rdp.cme.msu.edu/html/). Our sequence was aligned to these using CLUSTAL X (ref. 18) and the profile alignment option. Alignments were refined by eye using MacClade v. 4.03 (ref. 19).

Exclusion of unreliably aligned positions

To avoid subjectivity in excluding unreliably aligned positions from phylogenetic analyses, the program Gblocks version 0.91b (ref. 20) was used with the standard settings.

Phylogenetic reconstruction

Maximum likelihood (ML) tree estimation used PAUP*4.0b10 (ref. 12) and followed a previously described procedure[21]. PAUP* was also used for maximum parsimony and neighbour joining (NJ) using several methods for calculating the distance matrix.

We also used the MrBayes software[13] to estimate the best tree using bayesian inference of phylogeny. The gamma parameter with eight rate categories, proportion of invariant sites, GTR matrix and nucleotide frequencies were all estimated. Four chains were run with 1,000,000 generations. Every 100th tree was stored and their likelihoods plateaued after approximately 25% of the run. The last 100 trees (final 10%) were used to make a consensus tree in which the frequency of occurrence of each clade indicates the support for this clade.

Non-parametric bootstraps

NJML non-parametric bootstrapping (NJMLBP) was used to gauge support for relationships. For 1,000 bootstrapped data sets, an NJ tree was calculated from ML distances calculated using the gamma parameter (α) proportion of invariant sites (pinv) parameters fixed as calculated for the original data set based on the ML tree. Base frequencies and rate matrix values were estimated for each bootstrap replicate.

Alternative hypothesis testing with likelihood ratio tests

The Shimodaira–Hasegawa test implemented in PAUP* was used to test whether alternative topologies were significantly less well supported by the data than those found in our ML tree. The RELL approximation method was used with 1,000 bootstrap replicates.

Received 28 February; accepted 9 June 2003; doi:10.1038/nature01851.

1. Westblad, E. *Xenoturbella bocki* n.g, n.sp, a peculiar, primitive turbellarian type. *Ark. Zool.* **1,** 3–29 (1949).
2. Reisinger, E. Was ist *Xenoturbella*? *Z. Wiss. Zool.* **164,** 188–198 (1960).
3. Pedersen, K. J. & Pedersen, L. R. Fine-structural observations on the extracellular-matrix (ecm) of *Xenoturbella bocki* Westblad, 1949. *Acta Zool.* **67,** 103–113 (1986).
4. Franzen, A. & Afzelius, B. A. The ciliated epidermis of *Xenoturbella bocki* (Platyhelminthes, Xenoturbellida) with some phylogenetic considerations. *Zool. Scripta* **16,** 9–17 (1987).
5. Lundin, K. The epidermal ciliary rootlets of *Xenoturbella bocki* (Xenoturbellida) revisited: new support for a possible kinship with the Acoelomorpha (Platyhelminthes). *Zool. Scripta* **27,** 263–270 (1998).
6. Lundin, K. Degenerating epidermal cells in *Xenoturbella bocki* (phylum uncertain), Nemertodermatida and Acoela (Platyhelminthes). *Belg. J. Zool.* **131,** 153–157 (2001).
7. Pardos, F. Fine structure and function of pharynx cilia in *Glossobalanus minutus* Kowalewsky (Enteropneusta). *Acta Zool.* **69,** 1–12 (1988).
8. Ehlers, U. & Sopott-Ehlers, B. Ultrastructure of the subepidermal musculature of *Xenoturbella bocki*, the adelphotaxon of the Bilateria. *Zoomorphology* **117,** 71–79 (1997).

9. Norén, M. & Jondelius, U. *Xenoturbella*'s molluscan relatives… *Nature* **390,** 31–32 (1997).
10. Israelsson, O. …and molluscan embryogenesis. *Nature* **390,** 32 (1997).
11. Israelsson, O. New light on the enigmatic *Xenoturbella* (phylum uncertain): ontogeny and phylogeny. *Proc. R. Soc. Lond. B* **266,** 835–841 (1999).
12. Swofford, D. L. *Phylogenetic Analysis Using Parsimony (*and other methods) version 4* (Sinauer Associates, Sunderland, Massachusetts, 1998).
13. Huelsenbeck, J. P. & Ronquist, F. MRBAYES: Bayesian inference of phylogeny. *Bioinformatics* **17,** 754–755 (2001).
14. Lowe, T. M. & Eddy, S. R. tRNAscan-SE: A program for improved detection of transfer RNA genes in genomic sequence. *Nucleic Acids Res.* **25,** 955–964 (1997).
15. Telford, M. J., Herniou, E. A., Russell, R. B. & Littlewood, D. T. J. Changes in mitochondrial genetic codes as phylogenetic characters: two examples from the flatworms. *Proc. Natl Acad. Sci. USA* **97,** 11359–11364 (2000).
16. Castresana, J., Feldmaier-Fuchs, G. & Pääbo, S. Codon reassignment and amino acid composition in hemichordate mitochondria. *Proc. Natl Acad. Sci. USA* **95,** 3703–3707 (1998).
17. Gee, H. *Before the Backbone. Views on the Origin of Vertebrates* (Chapman and Hall, London, 1996).
18. Jeanmougin, F., Thompson, J. D., Gouy, M., Higgins, D. G. & Gibson, T. J. Multiple sequence alignment with Clustal X. *Trends Biol. Sci.* **23,** 403–405 (1998).
19. Maddison, D. R., Maddison, W. P. *MacClade 4: Analysis of Phylogeny and Character Evolution* (Sinauer Associates, Sunderland, Massachusetts, 2000).
20. Castresana, J. Selection of conserved blocks from multiple alignments for their use in phylogenetic analysis. *Mol. Biol. Evol.* **17,** 540–552 (2000).
21. Telford, M. J., Lockyer, A. E., Cartwright-Finch, C. & Littlewood, D. T. J. Combined large and small subunit ribosomal RNA phylogenies support a basal position of the acoelomorph flatworms. *Proc. R. Soc. Lond. B* **270,** 1077–1083 (2003).

Supplementary Information accompanies the paper on **www.nature.com/nature**.

Acknowledgements We thank M. Akam and R. Jenner for comments on the manuscript, I. Ruiz Trillo for sharing unpublished results, and the scientists of Kristineberg Marine Station for help in sample collection. We are grateful for support from the Wellcome Trust to M.J.T. and to D.T.J.L.

Competing interests statement The authors declare that they have no competing financial interests.

Correspondence and requests for materials should be addressed to M.J.T. (mt281@cam.ac.uk).
Newly determined sequences have been submitted to GenBank under accession numbers AY291292–AY291293.

Speciation by host switch in brood parasitic indigobirds

Michael D. Sorenson[1,2], Kristina M. Sefc[1] & Robert B. Payne[2,3]

[1]*Department of Biology, Boston University, Boston, Massachusetts 02215, USA*
[2]*Museum of Zoology and* [3]*Department of Ecology and Evolutionary Biology, University of Michigan, Ann Arbor, Michigan 48109, USA*

A growing body of empirical and theoretical work supports the plausibility of sympatric speciation[1–3], but there remain few examples in which all the essential components of the process are well understood. The African indigobirds *Vidua* spp. are host-specific brood parasites. Indigobird nestlings are reared along with host young, and mimic the mouth markings of their respective hosts[4–6]. As adults, male indigobirds mimic host song[4–7], whereas females use these songs to choose both their mates and the nests they parasitize[8]. These behavioural mechanisms promote the cohesion of indigobird populations associated with a given host species, and provide a mechanism for reproductive isolation after a new host is colonized. Here we show that all indigobird species are similar genetically, but are significantly differentiated in both mitochondrial haplotype and nuclear allele frequencies. These data support a model of recent sympatric speciation. In contrast to the cuckoo *Cuculus canorus*, in which only female lineages are faithful to specific hosts[9,10], host switches have led to speciation in indigobirds because both males and females imprint on their hosts[8,11].

The high degree of host specificity in indigobirds led previously to the suggestion that host–parasite associations in African finches were the product of a long history of co–speciation[4]. This model accounted for the remarkable mimicry of host mouth markings by the young parasites without requiring specialist parasites to have colonized hosts with different mouth markings. Genetic studies, however, indicate that indigobird species have a much more recent origin than their hosts[12,13]. Indeed, the lack of differentiation among indigobirds in mitochondrial DNA (mtDNA) restriction-fragment length polymorphism (RFLP) markers[12] is somewhat difficult to reconcile with their distinct behaviour[14] and morphology (Fig. 1). Behavioural imprinting in both males (song mimicry)[11] and females (mate choice, host choice)[8] suggests a mechanism for rapid sympatric speciation: indigobirds reared by a novel host species acquire the songs of that host and mate assortatively, resulting in immediate reproductive isolation after a new host is colonized. If this model is correct, the genetic similarity of indigobirds may be attributed to their recent origin from a common ancestor, but evidence of current reproductive isolation also is predicted. We tested this by comparing mitochondrial haplotype and nuclear microsatellite allele frequencies among seven indigobird species in West Africa (samples from Cameroon and Nigeria) and four species in southern Africa (samples from Zimbabwe, Zambia, Malawi and South Africa).

Figure 2 shows unrooted mtDNA haplotype trees for indigobirds. Species within each region share a set of closely related haplotypes, with overall diversity similar to that typically found within a single avian species. For example, a maximum divergence of 2.1% between

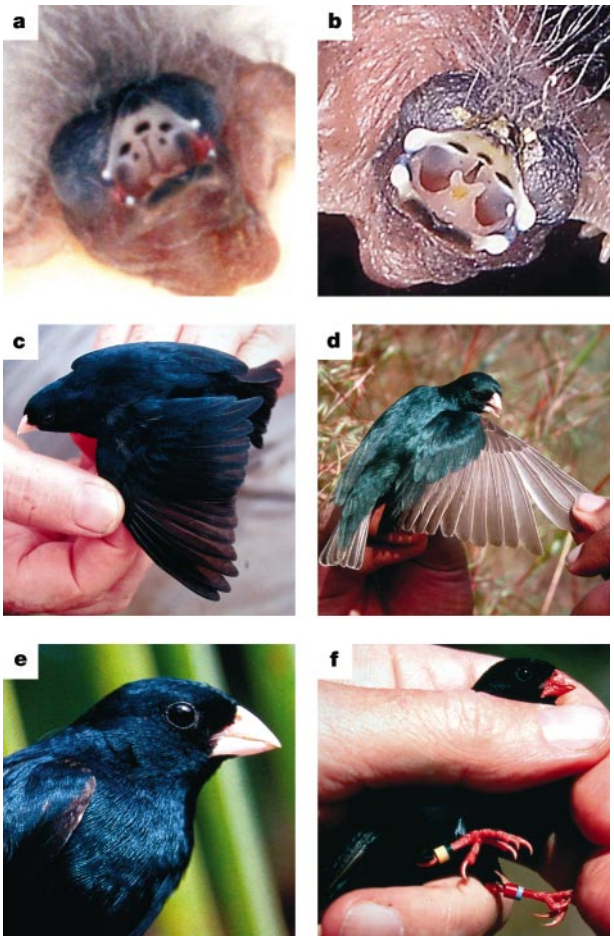

Figure 1 Examples of morphological variation between indigobird species. Nestling mouth markings in *V. camerunensis* (**a**) and *V. chalybeata* (**b**) mimic the young of their firefinch hosts, *L. rara* and *L. senegala*, respectively. Dark wing and plumage in *V. chalybeata* from West Africa (**c**). Pale wing and green plumage in *V. raricola* (**d**). White bill and blue plumage in *V. camerunensis* (**e**). Red bill and orange feet in *V. chalybeata* from southern Africa (**f**). See ref. 30 for a complete description of morphological differences between indigobird species.